AIAA JOURNAL
Vol. 47, No. 5, May 2009

Viscous Effects in Steady Reflection of Strong Shock Waves

Dmitry V. Khotyanovsky,* Yevgeniy A. Bondar,* Alexey N. Kudryavtsev,† Georgiy V. Shoev,‡ and Mikhail S. Ivanov§
Russian Academy of Sciences, 630090, Novosibirsk, Russia

DOI: 10.2514/1.40539

Regular and Mach reflections of shock waves from the symmetry plane in a steady Mach 4 flow of a monatomic gas have been numerically studied with the use of the continuum (Navier–Stokes) and kinetic (direct simulation Monte Carlo) simulations. Results of the computations demonstrate a prominent effect of flow viscosity and heat conduction in the vicinity of the shock intersection, where the flow parameters depart from the values prescribed by the inviscid theoretical solutions. The reasons for these discrepancies are discussed.

Nomenclature

g	=	distance from the trailing edge of the wedge to the plane of symmetry
Kn	=	Knudsen number
M	=	Mach number
p	=	pressure
Pr	=	Prandtl number
R	=	gas constant
Re	=	Reynolds number
T	=	temperature
w	=	length of the wedge along its windward side
α	=	shock angle of incidence
γ	=	heat capacity ratio
θ	=	angle of flow deflection
θ_w	=	wedge angle of attack
λ	=	mean free path
μ	=	dynamic viscosity
ω	=	exponent in power-law dependence of viscosity on temperature

Subscript

∞	=	freestream flow parameters

I. Introduction

STEADY shock wave reflections and interactions are very important in supersonic aerodynamics. Shock/shock interactions of various types can occur on supersonic and hypersonic aircraft during maneuvers and in cruise flight. Shock waves propagating from the nose of an aircraft can interact with shocks generated by other elements of the aircraft, such as wings, fins, inlet cowls, etc. Regular and irregular interactions of different types are inherent in such critical phenomena as off-design inlet flows and inlet starting.

Steady shock wave reflection has been extensively studied in recent years with an emphasis on strong shock waves, that is, at flow Mach numbers higher than 2.2 in air. This Mach number range is of primary importance for prospective hypersonic vehicles. These recent studies are mainly focused on the existence of two possible steady shock reflection configurations, regular and Mach reflections, in the dual solution domain, and the hysteresis phenomenon in the transition between them. A review of these studies can be found in [1]. Case distinction between weak and strong shock wave reflections is discussed in [2].

Classical theoretical methods such as the shock polar analysis and the three-shock theory based on Rankine–Hugoniot jump conditions across oblique shocks were developed by von Neumann [3] to describe shock wave configurations for various flow parameters and to predict transitions between different types of shock wave interaction. It is assumed that all shocks have negligible curvature and thickness. These theoretical methods predict well most of the features of shock wave interaction, at least for strong shocks. However, there are situations where the von Neumann theory fails. In reflection of weak shock waves (i.e., at flow Mach numbers lower than 2.2 in air), there is a range of flow parameters where the von Neumann three-shock theory does not produce any solution, whereas numerous experiments and numerical simulations (e.g., [4]) reveal a three-shock structure similar to the Mach reflection pattern. This inconsistency is usually referred to as the von Neumann paradox. One of the possible approaches to resolve the von Neumann paradox is to account for viscous effects in the vicinity of the triple point [5].

In reflection of strong shock waves the effects of flow viscosity and shock curvature manifest themselves in a small vicinity of shock intersection. These phenomena, however, may affect the transition between regular and Mach reflections for flow parameters corresponding to the dual solution domain, where both types of steady reflections are possible.

The structure of three-shock intersection in Mach reflection of strong shock waves was studied in [6] for a shock wave diffracting over a wedge, that is, in a pseudosteady case. The results of these shock tube experiments suggest the existence of a hot spot near the triple point. This conclusion was made based on the analysis of the schlieren photographs that showed some traces of the triple point trajectories. The inviscid computations clearly indicated the presence of spikes in temperature and pressure distributions immediately behind the triple point, a phenomenon that was not predicted by the three-shock theory. Unfortunately, the reason for the formation of these spikes could not be determined in [6] because the flowfield in the vicinity of the triple point was affected by the numerical dissipation inherent in any shock-capturing inviscid flow solver rather than by physical transport phenomena.

In this paper we study the reflection of strong shock waves with allowance for flow viscosity and heat conduction. The computations performed with the Navier–Stokes and the direct simulation

Presented as Paper 1187 at the 46th Aerospace Sciences Meeting and Exhibit, Reno, NV, 7–10 January 2008; received 8 September 2008; revision received 16 January 2009; accepted for publication 27 January 2009.

*Researcher, Khristianovich Institute of Theoretical and Applied Mechanics, Institutskaya 4/1.
†Senior Researcher, Khristianovich Institute of Theoretical and Applied Mechanics, Institutskaya 4/1.
‡Master of Science Student, Khristianovich Institute of Theoretical and Applied Mechanics, Institutskaya 4/1.
§Head of the Computational Aerodynamics Laboratory, Khristianovich Institute of Theoretical and Applied Mechanics, Institutskaya 4/1. Associate Fellow AIAA.

Monte Carlo (DSMC) flow solvers resolve the internal structure of shock waves and the region of shock intersection and, thus, can help clarify physical mechanisms that govern the flowfield close to the triple point.

II. Problem Formulation and Flow Conditions

We studied the reflection of an oblique shock wave with an angle of incidence α generated by a wedge in a steady flow with a Mach number $M = 4$ from the plane of symmetry as shown in Fig. 1. To eliminate possible effects of internal degrees of freedom, a flow of the monatomic gas argon with a ratio of specific heats $\gamma = 5/3$ and a Prandtl number $Pr = 0.66$ was considered. We examined two cases with wedge angles $\theta_w = 15$ deg (regular reflection, RR) and $\theta_w = 25$ deg (Mach reflection, MR) with the corresponding shock polar solutions shown in Fig. 2. In the first case, a reflected shock (RS) wave is formed at the intersection point of the incident shock IS and the plane of symmetry. The flow that passes through the RS returns to its original direction parallel to the freestream. The pressure behind the reflected shock corresponding to the intersection of the IS and RS polars is $p/p_\infty = 12.93$. The Mach number behind the reflected shock remains supersonic, and its theoretical value is $M = 1.725$. In the second case $\theta_w = 25$ deg, there is no regular solution, and an MR pattern is produced instead. The three-shock solution marked as MR in Fig. 2 predicts the values of pressure and flow deflection at the triple point $p/p_\infty = 19.57$ and $\theta = 12.42$ deg, respectively. A slipstream, that is, a contact discontinuity, emanates from the triple point T due to inequality of entropy in the flow passing through the incident and reflected shocks and the flow passing through the Mach shock. The flow behind the Mach shock is subsonic and is gradually accelerated back to supersonic speed owing to influence of expansion waves emanating from the trailing edge of the wedge and transmitted through the reflected shock. As a result, a closed subsonic pocket is formed behind the Mach stem. The size of the subsonic zone and, consequently, the position of the Mach stem are governed by the location of the leading characteristic of the expansion fan (EF), that is, depending on the geometry of the problem. The Mach number values behind the reflected shock and the Mach shock are, respectively, 1.151 and 0.5158. On the plane of symmetry, where the Mach stem is normal to the flow, the pressure behind the shock is $p/p_\infty =$ 19.75, and the corresponding Mach number value is 0.4904.

The length of the wedge w along its windward side was used as the characteristic length scale. The geometry of the problem is described by the parameter g/w, which is the normalized distance from the trailing edge of the wedge to the symmetry plane.

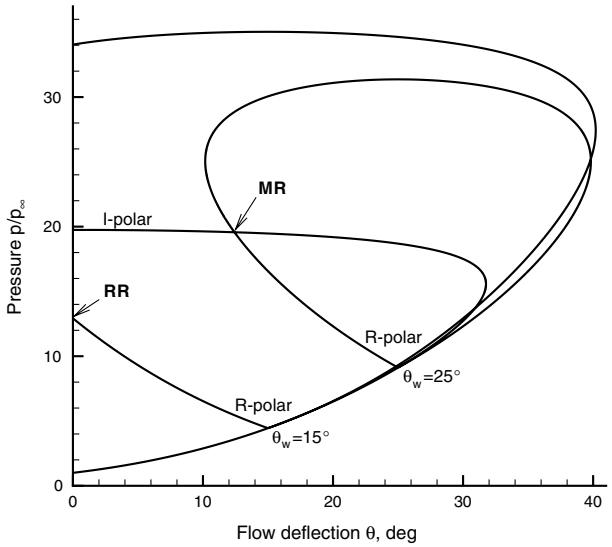

Fig. 2 Theoretical solutions for regular (RR) and Mach (MR) reflections in the (θ, p) plane at $M = 4$, $\gamma = 5/3$, and two wedge angles θ_w.

III. Numerical Techniques

The numerical study is conducted with the continuum and kinetic approaches. The continuum simulations are based on finite-difference solution of the full two-dimensional Navier–Stokes equations of a compressible gas. Kinetic simulations use the (DSMC) [7] for numerical solution of the nonlinear Boltzmann equation. The DSMC method uses model particles, each of which represent a large number of real molecules. The DSMC simulation involves molecular movement and collision stages. The movement of the model particles in physical space is simulated in a realistic manner solving the equations of motion for each particle, and intermolecular collisions and collisions with surfaces are described with the phenomenological models. The DSMC method is widely used for simulation of rarefied and near-continuum flows. Two different simulation approaches were used to ensure that the results of the computations represent physical phenomena and not a numerical artifact. The region of shock wave intersection (e.g., the triple point) is a zone for which the characteristic length scale is compared with the shock wave thickness [5], which is a few dozens of mean free paths λ. Because of the large gradients of the flow parameters and gas nonequilibrium inside the shock waves the applicability of the Navier–Stokes equations to describe the fluid dynamics within the shock intersection region cannot be taken for granted. It seems essential that the results of the Navier–Stokes computations be compared with the results obtained by the DSMC method, which uses a physically realistic approach for modeling the gas flow. Cross comparison of the results is also important because of the lack of the experimental data on the flow structure in the close vicinity of the shock intersection.

The Navier–Stokes code [8] is a time-explicit shock-capturing code based on fifth-order weighted essentially nonoscillatory reconstruction [9] of convective terms and a mixed, central-biased, fourth-order approximation of dissipation terms. The computations were run in a rectangular computational domain (see Fig. 3) with uniform grid spacing. The left boundary of the computational domain is a supersonic inflow with the freestream flow parameters imposed. The right boundary of the domain was placed far enough downstream to ensure supersonic outflow conditions there. Extrapolation of the flow variables was used to impose boundary conditions at the outflow. At the lower boundary of the domain, symmetrical boundary conditions (mirror reflection) were used. The upper boundary was placed at $y = g$ corresponding to the vertical

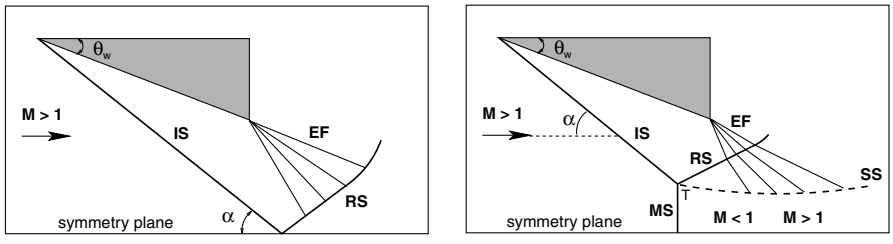

Fig. 1 Schematic of a) regular and b) Mach shock wave reflections where IS is incident shock, RS is reflected shock, MS is Mach shock, EF is expansion fan, SS is slipstream, and T is triple point.

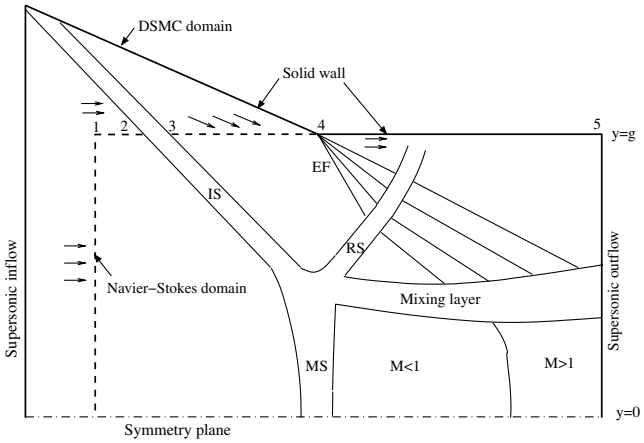

Fig. 3 Schematic of the Navier–Stokes and DSMC computational domains and boundary conditions where IS is incident shock, RS is reflected shock, MS is Mach shock, and EF is expansion fan.

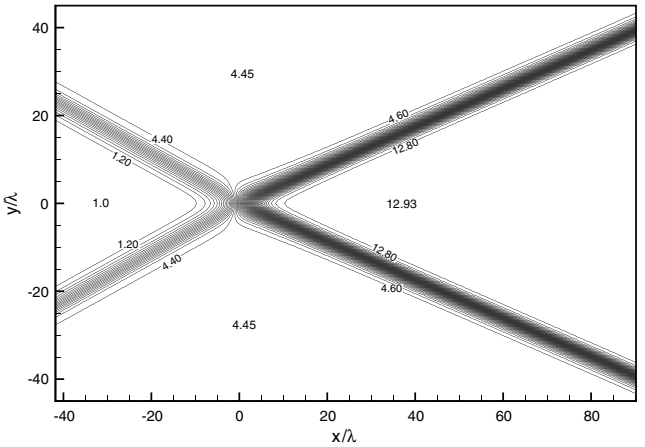

Fig. 4 Pressure contours for regular reflection at $M = 4$, $\gamma = 5/3$, and wedge angle $\theta_w = 15\,\mathrm{deg}$.

position of the trailing edge of the wedge. The boundary conditions on the upper boundary were specified in a complex manner to maintain flow conditions at the horizontal line $y = g$. Supersonic freestream conditions were specified along the segment 1–2 of the upper boundary (see Fig. 3). The segment 2–3 corresponds to the intersection of the upper boundary with the incident shock, where in the viscous case a smooth variation of the flow parameters inside the shock wave should be specified. For the internal structure of the shock wave we used the analytical solution of the one-dimensional Navier–Stokes equations that can be found in [10]. Along the line segment 3–4 the flow parameters corresponding to Rankine–Hugoniot conditions behind the incident shock were imposed. Along the segment 4–5 the inviscid wall (symmetry) boundary conditions were used. The computations were started with a uniform supersonic flow filling the entire computational domain. The numerical solution was then advanced in time with the second-order Runge–Kutta scheme until a steady state was achieved. Convergence to the steady state was established when the variation of the right-hand sides of the Navier–Stokes equations at a given time step in L_∞ and L_1 norms dropped below a certain small value. Additionally, the characteristic flow features, such as shock positions, were also monitored during the computations to ensure their time independence.

The DSMC simulations are performed with the SMILE code [11], which uses the majorant frequency method for computing collision

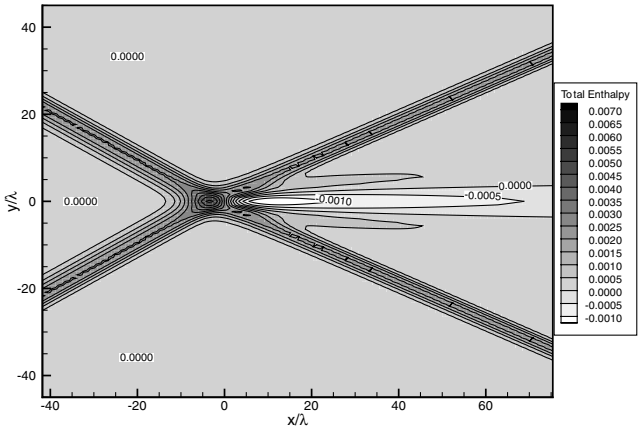

Fig. 5 Flowfield and contours of normalized total enthalpy $((h_t\text{-}h_{t\infty})/h_{t\infty}$ for regular reflection at $M = 4$, $\gamma = 5/3$, and wedge angle $\theta_w = 15\,\mathrm{deg}$.

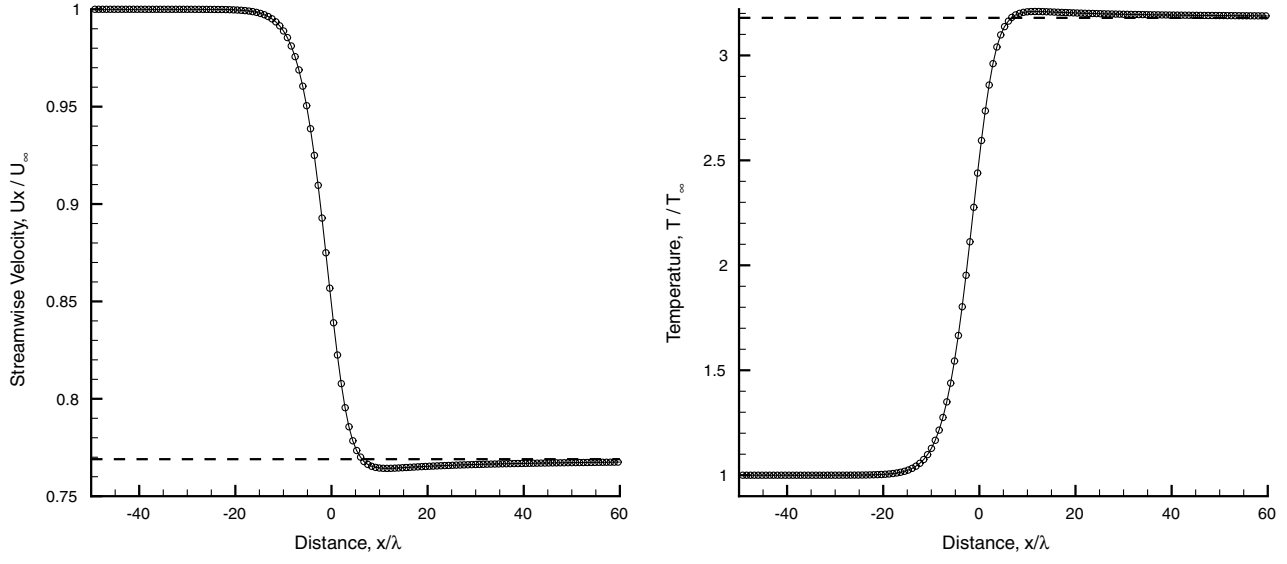

a) **b)**

Fig. 6 Distribution of a) streamwise velocity component and b) temperature along the symmetry plane for regular reflection. The dashed curve shows the theoretical values.

integrals. The computational domain was similar to the domain used in the Navier–Stokes computations (see Fig. 3). Separate rectangular grids were used for modeling molecular collisions and sampling the gas dynamic parameters. The first grid was uniform, and its linear size was less than the minimum value of the mean free path in the computational domain. The second grid was condensed in the zones of interest: the Mach stem and the point of the shock reflection from the symmetry plane for Mach and regular reflection, respectively. At the initial moment, the domain was populated by the model particles according to the Maxwell distribution function corresponding to the freestream parameters. Freestream conditions were imposed on the left boundary and on a portion of the upper boundary of the computational domain. The right (downstream) boundary was selected so that the flow there was supersonic. A specular reflection condition was used at the lower boundary (the symmetry plane), the wedge surface, and the part of the upper boundary ($y = g$).

The computations properly resolved the internal structure of the shock waves. A sequence of grids was used to perform a grid resolution study. It was found that the results were independent of grids if the value of the Reynolds number based on the grid cell size was in the range from 2 to 4.

The power-law dependence of the dynamic viscosity coefficient μ on temperature T with an exponent $\omega = 0.81$ was used in the Navier–Stokes computations. The variable hard-sphere model [7] (VHS) was used in the DSMC computations with the VHS parameter chosen to provide the same dependence of viscosity on temperature. The relation between the Reynolds and Knudsen numbers can be obtained from the formula for the mean free path λ in an equilibrium gas given in [7]. For the VHS model of intermolecular collisions λ can be written as

$$\lambda = \frac{2(5-2\omega)(7-2\omega)}{15\pi^{1/2}} \frac{\mu}{(2RT)^{1/2}\rho} \tag{1}$$

where R is the gas constant, T is the temperature, and ρ is the density. Then the relation between Kn and Re is

$$Kn = \frac{2(5-2\omega)(7-2\omega)}{15\pi^{1/2}} \left(\frac{\gamma}{2}\right)^{1/2} \frac{M}{Re} \tag{2}$$

The Reynolds number in the Navier–Stokes simulations and the Knudsen number in DSMC computations were varied in the course of our computational study.

IV. Regular Reflection

The flow structure of the regular reflection region obtained in the Navier–Stokes simulations at Reynolds number $Re = 1.0 \times 10^3$ is shown in Figs. 4 and 5. The problem of regular reflection has no length scale related to the wedge size (in contrast to Mach reflection where the size of the subsonic pocket behind the Mach stem is governed by the parameter g/w). In the following we will use the normalized coordinates x/λ and y/λ with the origin set at the reflection point. The latter is defined here as the point in the symmetry plane where the density reaches the value behind the incident shock. Flow viscosity causes the formation of a wake behind the regular reflection region where flow parameters differ from the prediction of the inviscid theory. This wake is isobaric, and so the pressure behind the reflection region coincides with the value $p/p_\infty = 12.93$ predicted by the shock polar solution. However, the flow inside the wake is apparently hotter and has lower velocity, which is evident in Fig. 6. This fact can be explained by the influence of the dissipation terms in the energy equation, which transfer part of the flow kinetic energy into heat. The phenomenon is illustrated in Fig. 5 as variation of the total enthalpy of the gas flow. The total enthalpy is normalized to its freestream value $h_{t\infty}$. As can be expected, h_t inside the shock waves is higher than its freestream value owing to nonequilibrium of dissipation and heat conduction. (Note, the present computations were performed for argon with a Prandtl number $Pr = 0.66$. Becker's constant-enthalpy solution [12] is valid for $Pr = 3/4$). Behind the planar portions of incident and reflected shocks h_t restores its freestream value to obey the Rankine–Hugoniot relations. Inside the wake, h_t falls below its freestream value due to excessive dissipation of the kinetic energy. The vertical size of the wake has the order of 10λ, that is, is comparable with the shock wave thickness.

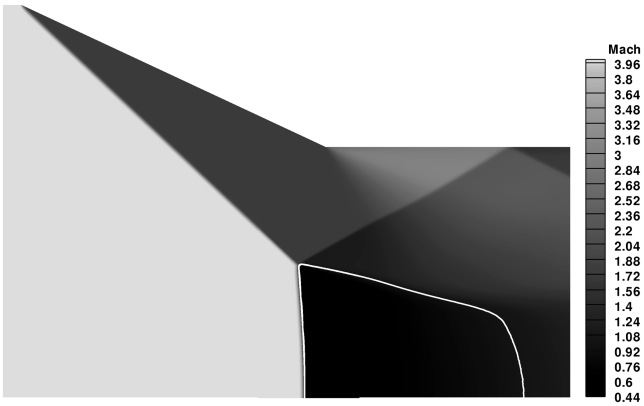

Fig. 7 Mach number flowfield for Mach reflection at $M = 4$, $\gamma = 5/3$, and wedge angle $\theta_w = 25$ deg obtained in DSMC computations at $Kn = 1.0 \times 10^{-3}$. The sonic line is shown in white.

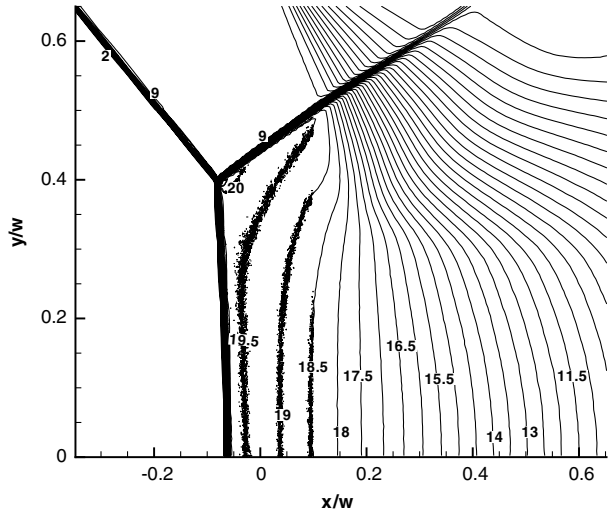

a)

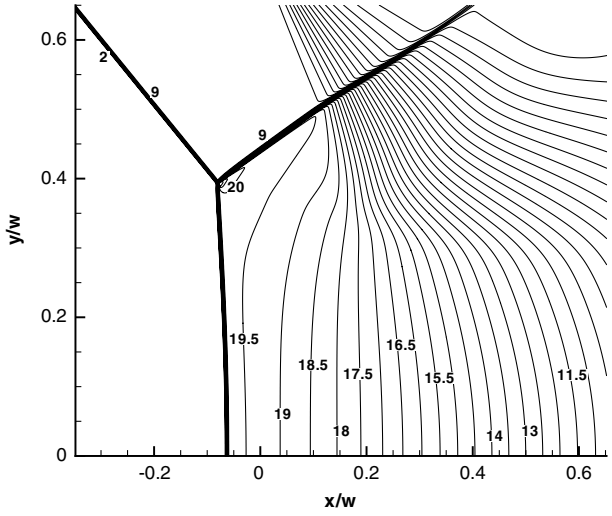

b)

Fig. 8 Pressure contours for Mach reflection at $M = 4$, $\gamma = 5/3$, and $\theta_w = 25$ deg obtained in DSMC computations at a) $Kn = 1.0 \times 10^{-3}$ and b) corresponding Navier–Stokes computations at $Re = 5 \times 10^3$.

Farther downstream, due to laminar mixing in the wake boundary layers, the wake is gradually equalized with the external flow, and the flow parameters tend to the values prescribed by the two-shock solution. However, the presence of the wake is still observed at the downstream boundary of the domain, which is located at $x/\lambda = 250$.

The results of our additional computations, not presented here, performed with the Navier–Stokes code at $Pr = 3/4$, that is, in a constant-total-enthalpy case, have shown a far less pronounced effect. In this case, the total enthalpy and temperature slightly increase in the plane of symmetry behind the reflection region, whereas the pressure and velocity coincide with the values prescribed by the inviscid solution.

V. Mach Reflection

The Mach number flowfield for Mach reflection at $\theta_w = 25$ deg is shown in Fig. 7. The overall flow structure is similar to the conventional inviscid Mach reflection pattern. The results shown in the figure clearly display a closed subsonic pocket behind the Mach stem. As mentioned in Sec. II, the expansion waves of the EF centered at the trailing edge of the wedge provide necessary flow acceleration (see flow schematics in Figs. 1b and 3). Expansion waves are transmitted through the RS and interact with the slipstream (with the mixing layer in a viscous case) inducing negative pressure gradient in streamwise direction. As a result, a virtual converging–diverging nozzle is formed by the curved mixing layer. The initial subsonic flow behind the Mach stem is accelerated in this virtual nozzle to a supersonic velocity. The results of the computations presented in this section were obtained for a geometrical parameter $g/w = 0.75$. Figure 8 is an enlarged view of the flowfields near the three-shock intersection obtained by the DSMC method at a Knudsen number $Kn = 0.001$ and the corresponding Navier–Stokes solution at a Reynolds number $Re = 5.0 \times 10^3$. According to the three-shock theory, the pressure behind the reflected shock and Mach stem should be equal to $p/p_\infty \approx 19.57$ in this case, but the computations reveal an elevated pressure region with a maximum value $p/p_\infty \approx 21$. The presence of such a high-pressure spot behind the triple point is consistent with the results of Euler simulations [6] discussed in Sec. I, but in our case it is the effect of physical rather than numerical dissipation. The results of DSMC and Navier–Stokes computations are very close to each other (cf. Figs. 8a and 8b), so that specific pressure contours become indistinguishable if the two flowfields are overlaid. A detailed comparison of these numerical results with the theoretical predictions is given in Fig. 9, where the

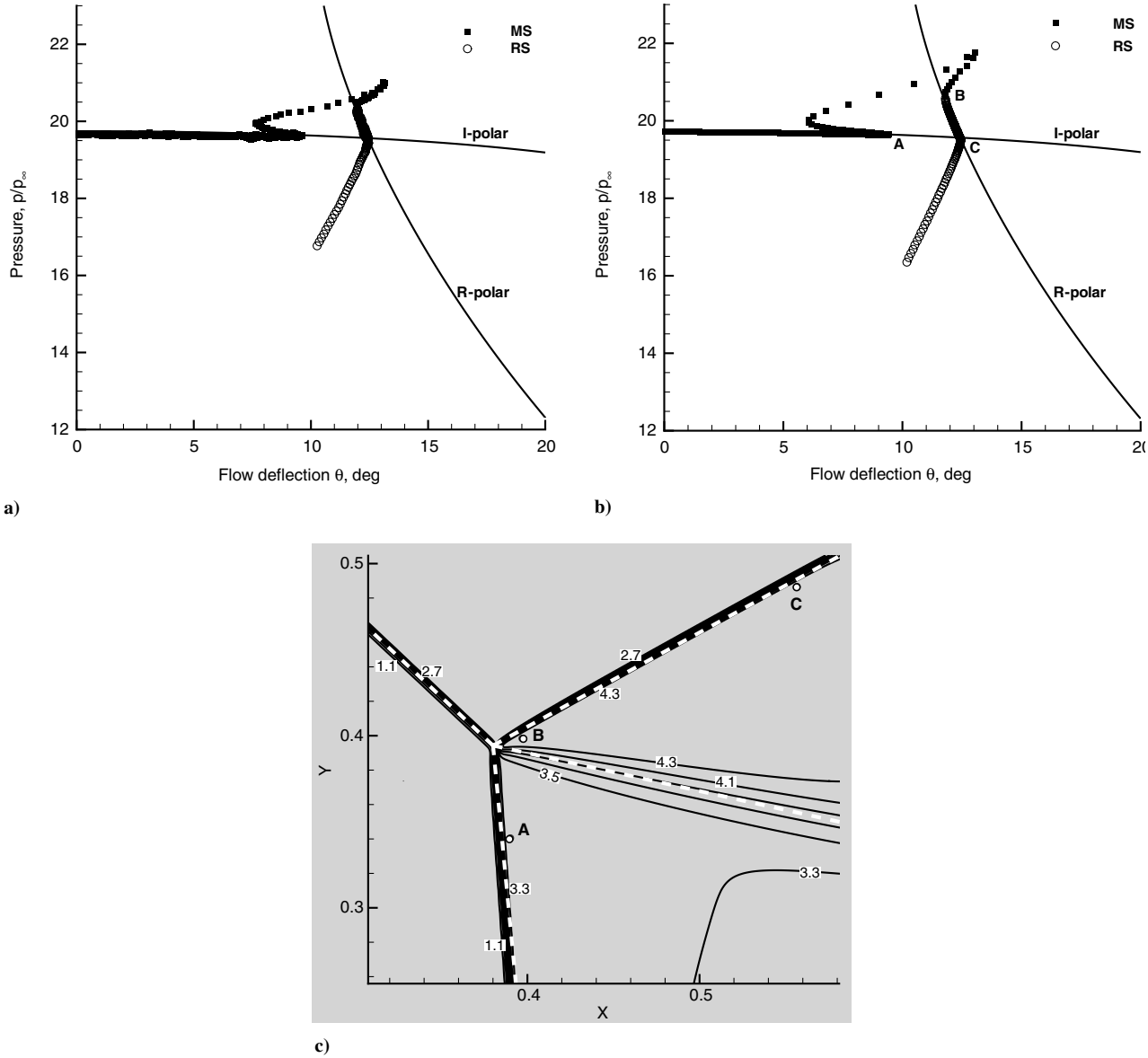

Fig. 9 Flow conditions behind the MS and RS waves in the (θ, p) plane at $M = 4$, $\gamma = 5/3$, and $\theta_w = 25$ deg obtained in a) DSMC computations at $Kn = 1.0 \times 10^{-3}$ and b) corresponding Navier–Stokes computations at $Re = 5 \times 10^3$; c) density contours in the Navier–Stokes computations (white dashed lines correspond to theoretical orientations of the shock waves and slipstream).

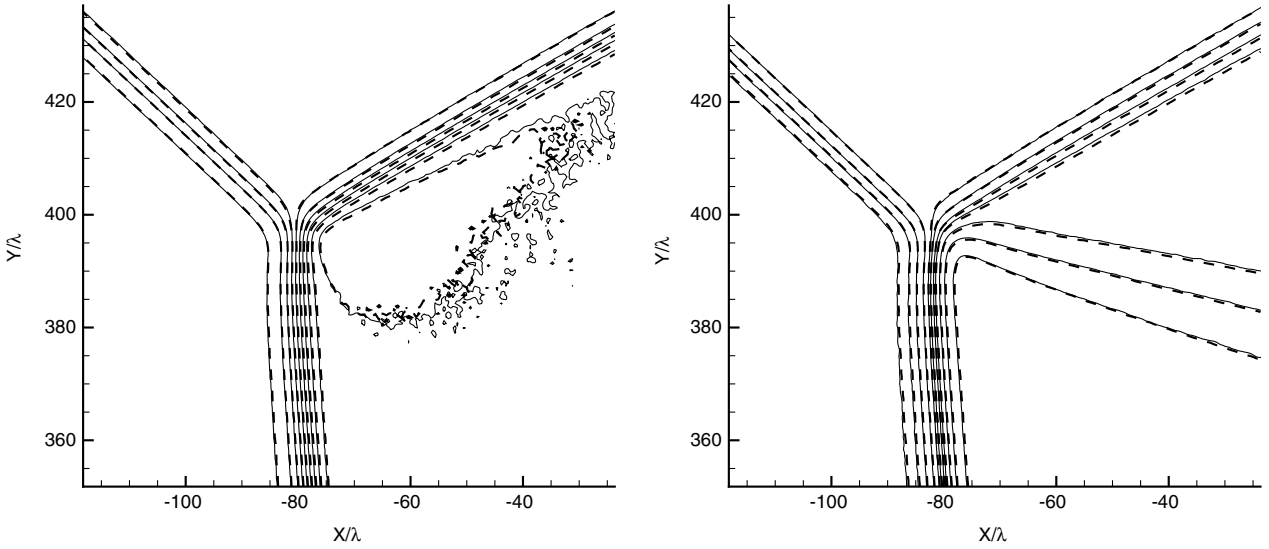

Fig. 10 Flow structure near the three-shock intersection obtained in DSMC computations at $Kn = 1.0 \times 10^{-3}$ (dashed curves) and $Kn = 5 \times 10^{-4}$ (solid curves) showing a) pressure contours and b) Mach number contours.

values of pressure and flow deflection angle θ extracted from the numerical flowfields immediately behind the Mach stem and the reflected shock are plotted against the analytical shock polar solution in the (θ, p) plane. The values were taken along the contour, at which the pressure gradient was equal to 1–5% of its maximum value inside the shock. It is seen from Fig. 9 that the numerical values deviate from the theoretical polar, beginning from a certain angle of flow deflection $\theta \approx 8$ deg. The maximum pressure is greater than the pressure predicted by the three-shock theory by 8% for the DSMC calculation and by 12% for the Navier–Stokes equations. The maximum angle of flow deflection exceeds its value predicted by the three-shock theory for both DSMC and Navier–Stokes computations. As can be seen in Fig. 9, the portion of the Mach shock below point A is perfectly described by the incident shock polar: the numerically obtained values of pressure and flow deflection are very close to the incident shock polar. Though the Mach shock angle to the oncoming flow is continuously changing, the shock curvature is negligible, and the flow parameters obey the Rankine–Hugoniot relations. The same applies to the B–C portion of the reflected shock, where the numerically obtained values of pressure and flow deflection are very close to the reflected shock polar. The portion of the reflected shock that is higher than point C lies in the region where the reflected shock is influenced by the expansion waves propagating from the trailing edge of the wedge. The shock intersection region between point A on the Mach shock and point B on the reflected shock is not governed by the Rankine–Hugoniot relations and produces excessive pressure. The flowfield between points A and B may be termed as a non-Rankine–Hugoniot zone. This term was introduced in [5] to explain the existence of the irregular shock wave configuration under the von Neumann paradox conditions. As the present study shows, such a viscous transition zone is also observed in reflection of strong shock waves, where the three-shock solution exists.

It is well known that the spatial scales of viscosity, including the width of the shock, are determined by the mean free path of molecules in the gas. To analyze the effect of viscosity on the flow structure in the vicinity of the triple point, we compared the flowfields for different Knudsen numbers in coordinates normalized to the mean free path in the freestream: x/λ and y/λ. Figure 10 shows the pressure and Mach number in the vicinity of the triple point in normalized coordinates for Knudsen numbers $Kn = 1.0 \times 10^{-3}$ and $Kn = 5 \times 10^{-4}$. The origin of both coordinates was shifted to the center point of the three-shock intersection. The pressure and Mach number contours coincide in the vicinity of the triple point, which means that the flows in normalized coordinates are similar. As seen in the pressure field, the x and y sizes of the region with $p/p_\infty > 20$ exceed 30λ.

The observed region with an excessive pressure behind the three-shock intersection may be attributed to the deviation of the angles of the reflected and Mach shocks from the values prescribed by the three-shock theory. Such a deviation may be caused by flow displacement in the mixing layer issuing from the triple point. An analysis of these effects was made in [13]. The slipstream is considered as a laminar shear layer for which the thickness grows as the square root of the downstream distance. As a result, the streamlines are displaced, and the flow deflections behind the reflected shock and the Mach stem differ from their inviscid counterparts. At a certain characteristic distance downstream, the slope of the slipstream boundary can be evaluated on the basis of the boundary layer theory, and the corresponding corrected flow deflections and shock wave angles can be obtained. Such a correction qualitatively agrees with the numerically observed deviations of the pressure and flow deflection. In this formulation, the reflected shock and the Mach shock have higher intensities compared with the three-shock solutions and produce higher pressures behind the shock intersection.

VI. Conclusions

Regular and Mach reflections of shock waves from the symmetry plane in a steady Mach 4 flow of argon have been numerically studied with Navier–Stokes and direct simulation Monte Carlo flow solvers with resolution of the internal structure of shock waves. For regular reflection, the results of the computations demonstrate the formation of a wake behind the reflection region, a phenomenon that is not described by the inviscid theory. The gas inside the wake has a higher temperature and a lower velocity than the external flow outside the wake. The reason is excessive dissipation in the shock reflection region, some part of the flow kinetic energy being converted into heat, which is evident from the total enthalpy distributions. The wake thickness is comparable with the shock wave thickness. Downstream of the reflection point the wake flow is gradually equalized with the external flow, but its influence is observed up to the right boundary of the domain, which is located 250 mean free paths downstream.

In the Mach reflection case, the results of the computations show that flow viscosity and heat conduction strongly affect the triple point region, where the numerical solutions of the Navier–Stokes and Boltzmann equations depart from the values prescribed by the three-shock theory. This is manifested in the formation of a high-pressure spot behind the region of three-shock intersection. The size of this

region has the order of the shock wave thickness and increases with increasing flow viscosity. The flowfields in the vicinity of the triple point obtained at different Knudsen numbers coincide, if plotted in coordinates normalized to the freestream mean free path. A possible mechanism of the pressure increase can be the slipstream displacement in the mixing layer, providing higher intensities of the reflected and Mach shocks.

Acknowledgments

This research was supported by Russian Foundation for Basic Research projects 06-08-00687 and 06-01-22000 and the Fundamental Research Program 14 of the Russian Academy of Sciences. This support is gratefully acknowledged. The computations were performed at the Siberian Supercomputer Center, Novosibirsk, Russia, and the Joint Supercomputer Center, Moscow.

References

[1] Ben–Dor, G., "Oblique Shock Wave Reflections," *Handbook of Shock Waves*, edited by G. Ben-Dor, O. Igra, and E. Elperin, Academic Press, New York, Vol. 2, 2001, Chap. 8.

[2] Hornung, H., "Regular and Mach Reflection of Shock Waves," *Annual Review of Fluid Mechanics*, Vol. 18, No. 1, 1986, pp. 33–58. doi:10.1146/annurev.fl.18.010186.000341

[3] von Neumann, J., "Oblique Reflection of Shock Waves," Navy Department Bureau of Ordonance, Explosive Research Rept. 12, Washington D.C. 1943; also reprinted in *Collected Works of J. von Neumann*, Vol. 6, Pergamon Press, New York, 1963, pp. 238–299.

[4] Colella, P., and Henderson, L. F., "The von Neumann Paradox for the Diffraction of Weak Shock Waves," *Journal of Fluid Mechanics*, Vol. 213, 1990, pp. 71–94. doi:10.1017/S0022112090002221

[5] Sternberg, J., "Triple-Shock-Wave Intersections," *Physics of Fluids*, Vol. 2, No. 2, 1959, pp. 179–206. doi:10.1063/1.1705909

[6] Ben–Dor, G., Takayama, K., and Needham, C. E., "The Thermal Nature of the Triple Point of a Mach Reflection," *Physics of Fluids*, Vol. 30, No. 5, 1987, pp. 1287–1293. doi:10.1063/1.866243

[7] Bird, G., *Molecular Gas Dynamics and the Direct Simulation of Gas Flows*, Oxford Press, Oxford, England, U.K., 1994.

[8] Kudryavtsev, A. N., and Khotyanovsky, D. V., "Numerical Investigation of High Speed Free Shear Flow Instability and Mach Wave Radiation," *International Journal of Aeroacoustics*, Vol. 4, Nos. 3–4, 2005, pp. 325–344. doi:10.1260/1475472054771394

[9] Jiang, G., and Shu, C.-W., "Efficient Implementation of Weighted ENO Schemes," *Journal of Computational Physics*, Vol. 126, 1996, pp. 202–228. doi:10.1006/jcph.1996.0130

[10] Hayes, W. D., "The Basic Theory of Gasdynamic Discontinuities," *Fundamentals of Gas Dynamics*, edited by H. W. Emmons, High Speed Aerodynamics and Jet Propulsion, Princeton Univ. Press, Princeton, NJ, Vol. 3, 1958, Chap. 4.

[11] Ivanov, M. S., Markelov, G. N., and Gimelshein, S. F., "Statistical Simulation of Reactive Rarefied Flows: Numerical Approach and Applications," AIAA Paper 98-2669, 1998.

[12] Becker, R., "Stosswelle und Detonation," *Zeitschrift fur Physik*, Vol. 8, No. 1, 1922, pp. 321–362. doi:10.1007/BF01329605

[13] Ben–Dor, G., "A Reconsideration of the Three-Shock Theory for a Pseudo-Steady Mach Reflection," *Journal of Fluid Mechanics*, Vol. 181, 1987, pp. 467–484. doi:10.1017/S0022112087002179

K. Powell
Associate Editor